Loch Melfort Oyster Larvae Modelling

Dr Tom Scanlon, Dr Matt Stickland

MTS-CFD Limited

Email: mtscfd@gmail.com

Web: www.mts-cfd.com

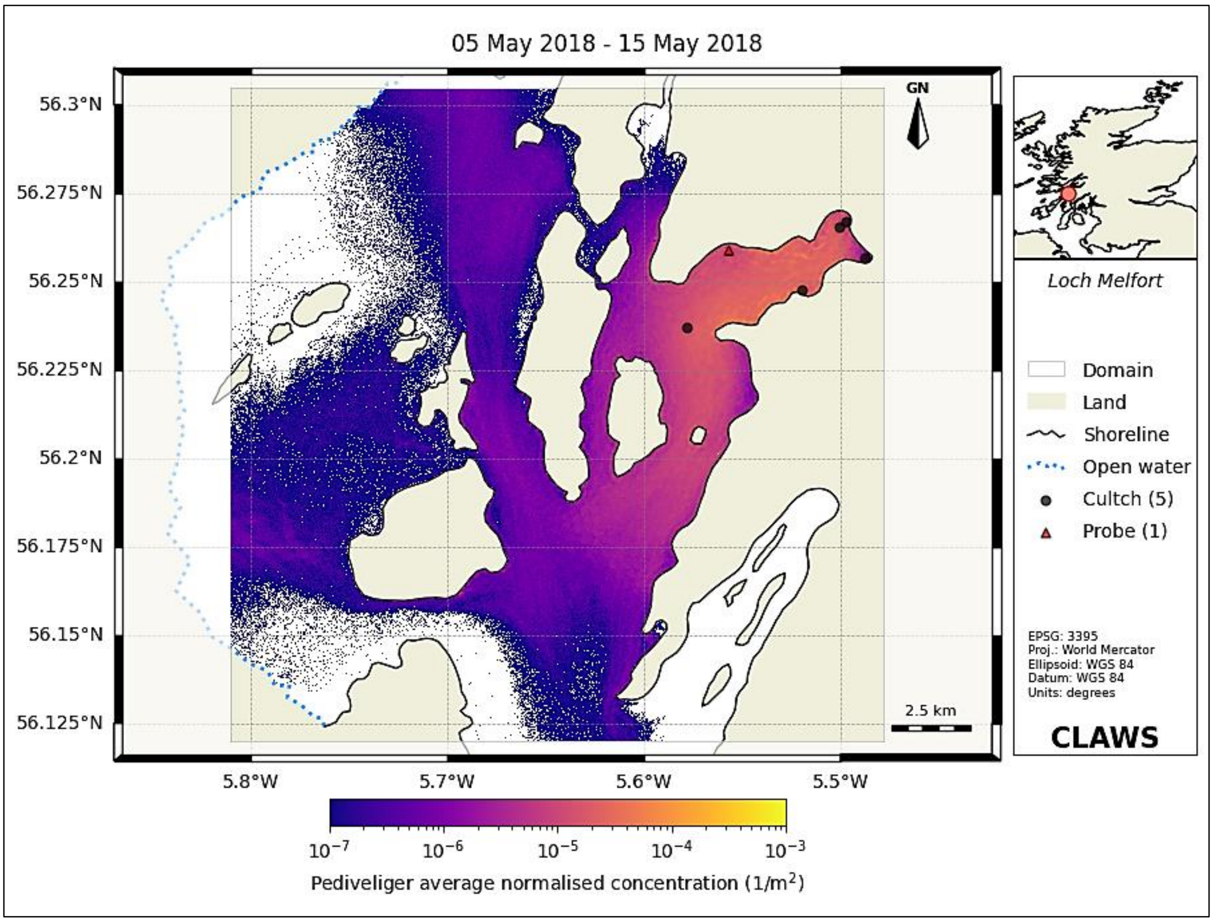

Executive Summary

A multi-stage biological model of oyster larvae (*Ostrea edulis*) has been developed in order to assess their distribution from 5 release sites in Loch Melfort. Tidal, wind and freshwater inflow conditions for May 2018 were considered in a 3D model of the sea loch.

Virtual "oyster larva" particles were released at each of the 5 sites and allowed to disperse into the marine environment. Particles were introduced into the model continuously at a rate of 20 per hour from each of the 5 sites over the 14-day run period. Each release zone was set as a volume of radius 10 m and depth of 1 m with particles placed randomly within the volume.

Each particle represents a single oyster larva and there were approximately 28,000 particles in the system at the end of the 14-day calculation. The model has the ability to prescribe multiple biological stages (trochophore, veliger and pediveliger), adjust swimming speed and direction, account for seafloor deposition and resuspension, larvae mortality and alteration of swim behaviour based on environmental cues such as changes in salinity. Output is in the form of heat maps of oyster larvae deposition density (#/m^2), larvae distribution in the water column and transport success (percentage of particles released from a site that deposit successfully).

The flow conditions (sea loch currents) driving the oyster larva particles come from a validated hydrodynamic model that has been reported elsewhere [CLAWS_2024] and is presented in summarised form in this document.

Results for the oyster larvae model show that the average pediveliger deposition concentrations in Loch Melfort are distributed widely across the loch and beyond with significant numbers of larvae observed to exit the loch into the surrounding area. The degree of transport success is predicted to be approximately 50% on average across the 5 release sites.

About the Report Authors

***Dr Tom Scanlon** BEng PhD CEng MIMechE, Engineering Consultant, MTS-CFD.com*

Tom is a chartered professional engineer with over 25 years' experience in applied computational mechanics. After a first degree in Environmental Engineering at the University of Strathclyde, Tom undertook a Ph.D in Vortex Shedding Flowmeter Pulsating Flow Computational Fluid Dynamics (CFD) Studies at the same university. Subsequently, he was awarded a JM Lessels scholarship from the Royal Society of Edinburgh for a one-year post-doctoral position at the Institute de Mécanique des Fluides de Toulouse, France in the field of numerical oceanography. The ImechE presented Tom with the Alfred Rosling Bennett Premium and Charles S Lake Award in 2003 for CFD in applied aerodynamics. In 2013 Tom returned from an EPSRC-funded sabbatical in the USA, where he carried out fundamental research in rarefied gas dynamics at the University of Michigan and the Lawrence Berkeley Laboratory in California. From 1994-2017 he was a Senior Lecturer in the Department of Mechanical and Aerospace Engineering at the University of Strathclyde specialising in heat transfer, fluid mechanics and applied CFD. His work is reported in over 50 refereed journal and conference publications. He is currently a director at the engineering consultancy firm MTS-CFD.

***Dr Matt Stickland** BSc PhD CEng FIMechE, Engineering Consultant, MTS-CFD.com*

After a first degree in Aeronautical Engineering at the University of Manchester, Matt worked for BAE Systems (Military Aircraft) at Warton in Lancashire in the Wind Tunnel Department working on projects which included EAP, EFA (Typhoon), Tornado and HOTOL. After leaving BAE in 1990 Matt worked for YARD Consulting Engineers in Glasgow modelling the heat and fluid flows in Advanced Gas Cooled reactors during on-load refuelling. In 1991 Matt accepted a senior lectureship in the Department of Mechanical Engineering at the University of Strathclyde where his research interest covered both experimental and computational heat transfer and fluid dynamics. He was awarded a PhD for his research into 3D imaging and its application to fluid flow visualisation. For his research in the field of experimental and computational fluid dynamics he was awarded the 2003 AR Bennett Premium/CS Lake Award and the 2004 T A Stewart-Dyer Prize/Frederick Harvey Trevithick Prize from the Institute of Mechanical Engineers. In 2022 Matt left the University of Strathclyde to take a directorship with the Engineering consultancy firm MTS-CFD. Matt is a Chartered Engineer and a Fellow of the Institute of Mechanical Engineers. He has published his research in over 100 papers in refereed journal and conference proceedings.

1 Introduction and Motivation

Rewilding efforts in Scottish sea lochs and estuaries have seen a significant focus on the restoration of native oyster populations, particularly the European flat oyster (*Ostrea edulis*). These initiatives aim to rejuvenate marine biodiversity, enhance water quality, and support local ecosystems. One notable project is taking place in Loch Craignish, where the charity Seawilding has been actively involved in reintroducing native oysters since 2020. Similarly, Loch Melfort is part of broader restoration efforts aimed at creating sustainable marine habitats and promoting ecological resilience. These projects not only strive to bring back the once-abundant oyster populations but also seek to foster a greater understanding and appreciation of marine conservation among local communities.

In order to assess the distribution of oyster larvae from 5 release sites in Loch Melfort, the Kilchoan Melfort Trust has commissioned the development of a detailed hydrodynamic and biological model of the area. The model simulates water levels and flows (i.e., currents and tides), which govern the transport and fate of oyster larvae emanating from the release sites – see [CLAWS_2024] for further details of the hydrodynamic model.

The use of hydrodynamic modelling to drive particles representing marine zooplankton is increasingly common [Johnsen_2020], [Asplin_2020], [Smyth_2016], [North_2008]. Marine Scotland and SEPA [SEPA_2024] are working on similar projects in Scotland. The integrated biological model presented in this report draws on the methods and assumptions used by Scottish and Norwegian modellers working for government agencies, as well as other peer-reviewed research.

In order to represent the oyster larvae, virtual "larva" particles were released at each of the 5 sites and allowed to disperse into the marine environment. Each particle represents a single larval stage. A modelling technique similar to the current SEPA screening approach [SEPA_2024] for salmon lice has been adopted, where the biological effects of oyster larvae production, maturity and mortality have been included. Larval swimming behaviour was also included in the model based on the criteria presented in [North_2008].

In this report the model outputs are presented in three ways, to categorise how the oyster larvae are likely to be distributed throughout Loch Melfort:

1. Oyster larvae deposition density (#/m^2) for pediveligers averaged over an 11-day period in May 2018, shown as a heat map.
2. Oyster larvae density (#/m^2) in the water column averaged over an 11-day period in May 2018, shown as a heat map.
3. A graph of transport success for larvae released from each of the 5 sites. Transport success is defined as the percentage of all particles released from a site that successfully deposit on the sea floor as pediveligers.

Animations of the larvae transport are also available as part of this study.

2 Hydrodynamic model

2.1 *Reduction of the full West Coast model*

The flow conditions (sea loch currents) that drive the oyster larva particles come from a validated hydrodynamic model that has been reported elsewhere [CLAWS_2024]. The extent of this full “West Coast” model is shown in Figure 1. The model has been developed by MTS-CFD to assess the impact of aquaculture-derived sea lice on wild Atlantic salmon and sea trout. The hydrodynamic model contains the influence of wind forcing on the loch surface and stratification through the salinity and temperature fields. It offers general insight into the spatial and temporal variation in the flow environment around the West Coast of Scotland and the hydrodynamic model also provides a suitable basis for modelling oyster larvae dispersion.

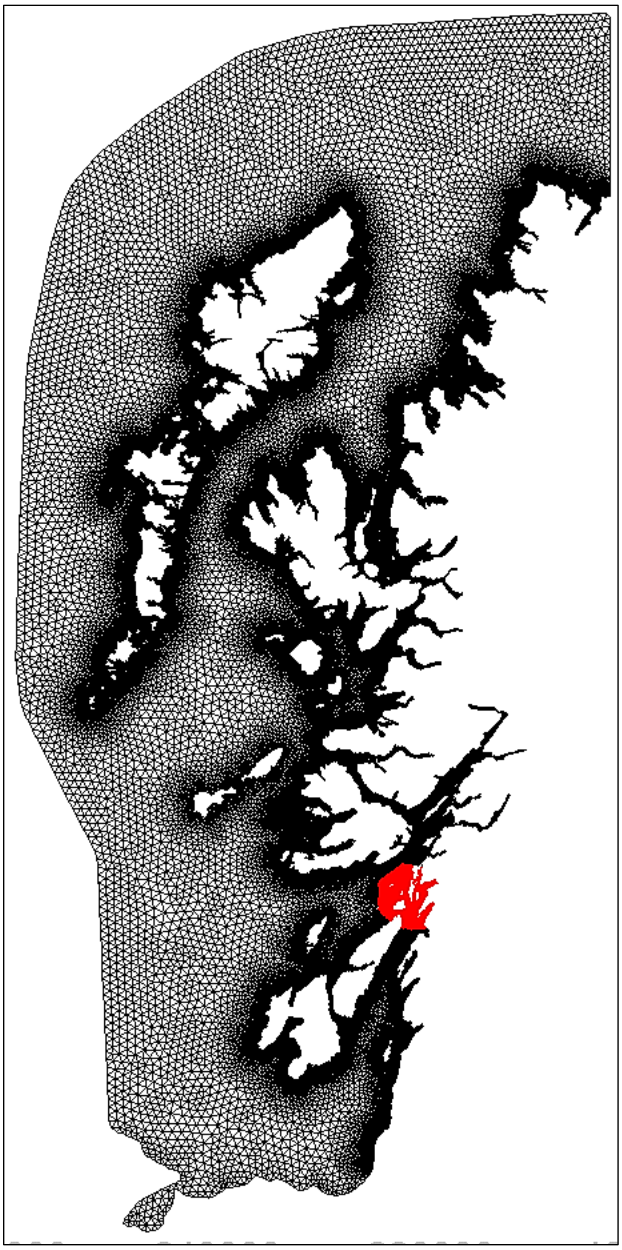

Figure 1 *Computational domain for the hydrodynamics of the West Coast of Scotland. Red zone highlights the sub-model area for Loch Melfort.*

In order to reduce the size of the West Coast model to one more focused on Loch Melfort, a subsection of the mesh around the area of interest is created and a hydrodynamic sub-model is created. The resulting mesh is shown in red in Figures 1-3.

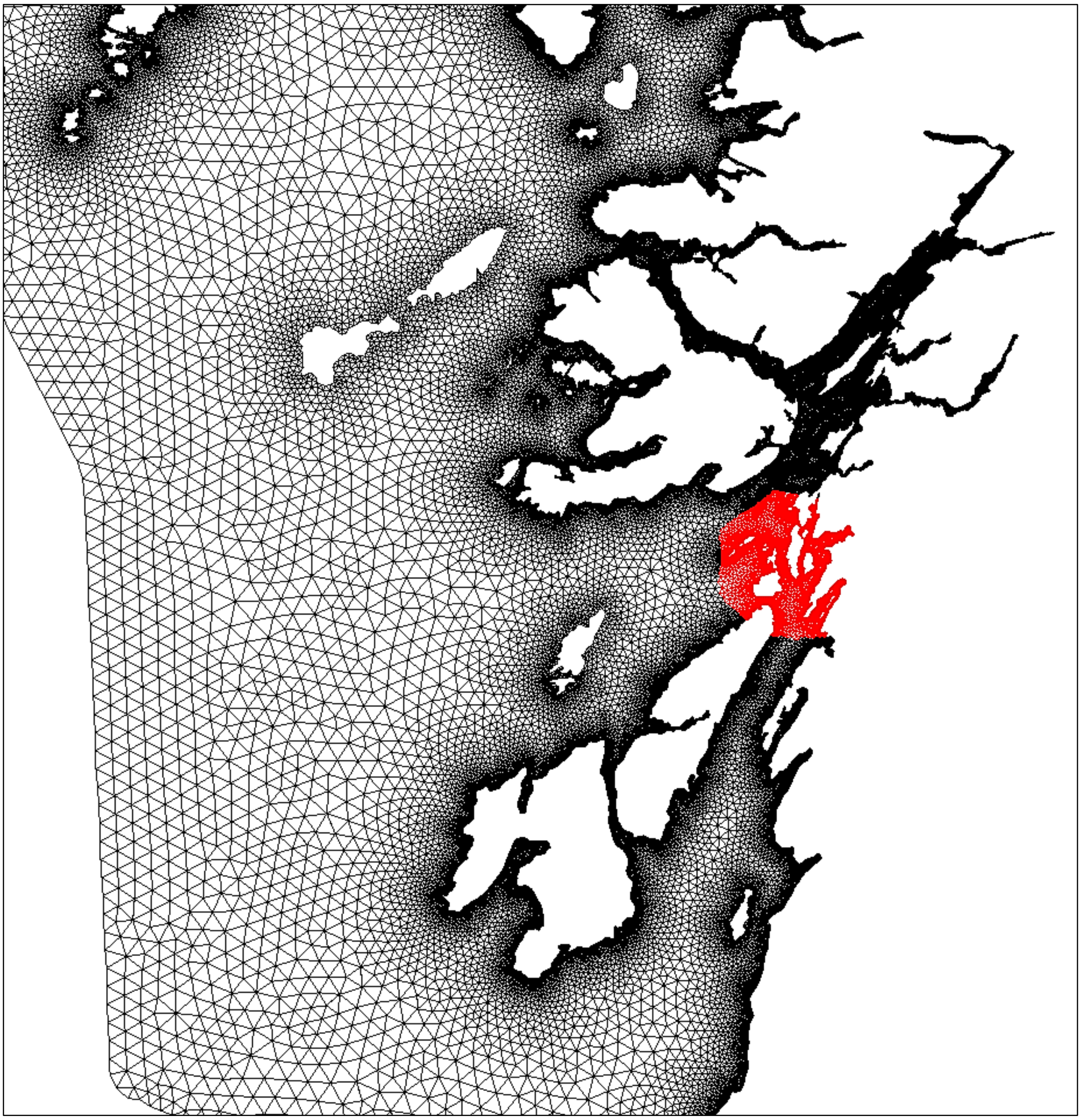

Figure 2 *Zoomed hydrodynamics mesh of the West Coast of Scotland. Red zone highlights the sub-model area for Loch Melfort.*

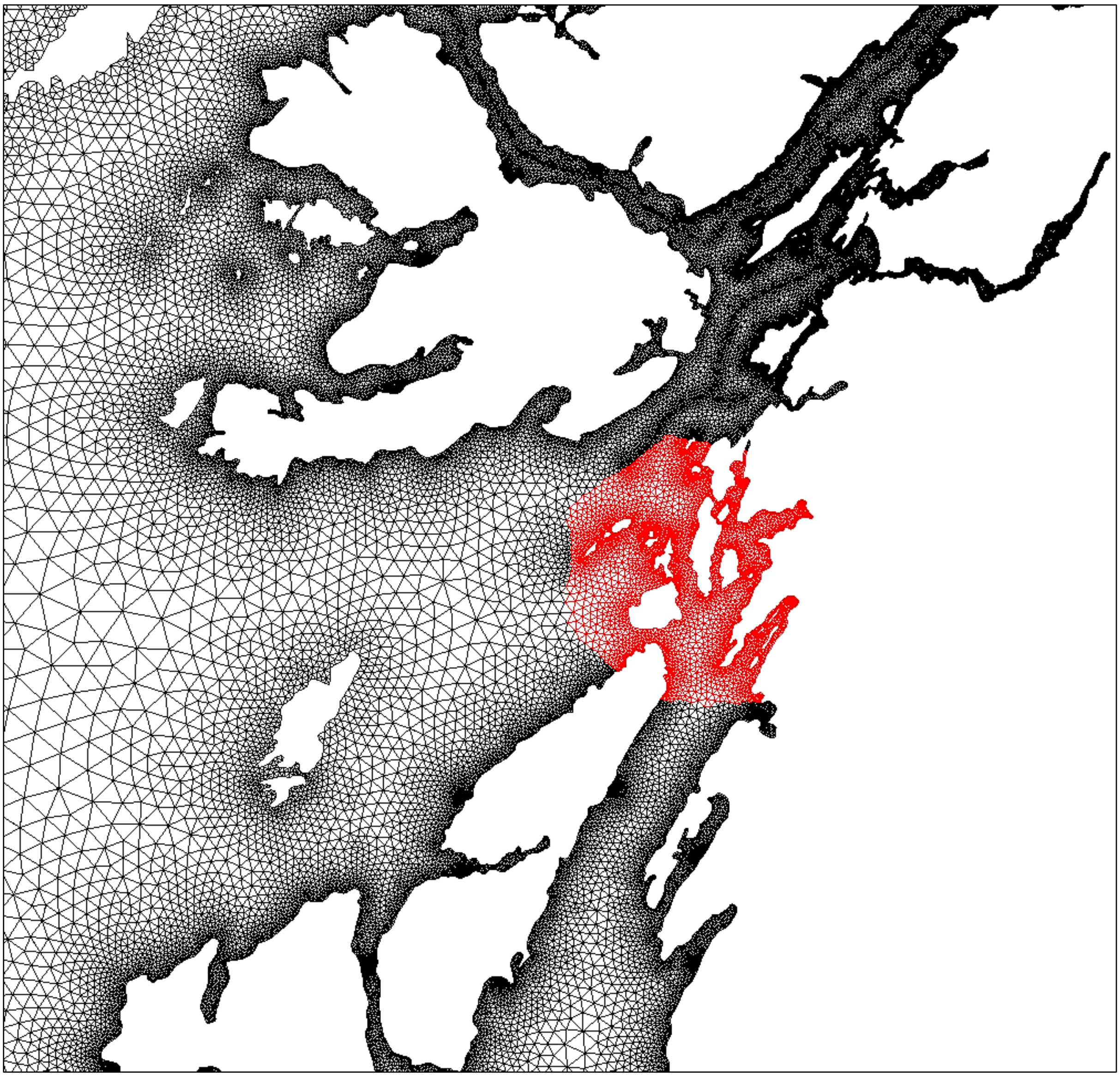

Figure 3 *Further-zoomed hydrodynamics mesh of the West Coast of Scotland. Red zone highlights the sub-model area for Loch Melfort.*

2.2 *Bathymetry*

The bathymetry data for the hydrodynamics model have been collected from a range of different sources including publicly available data sets provided by Marine Scotland for the Scottish Shelf Model [SSM_2024], digitised Admiralty charts and bathymetry information from the UK's Digimap Ordnance Survey Collection [DOSC_2023]. The bathymetry in the local area is shown in Figures 4 and 5.

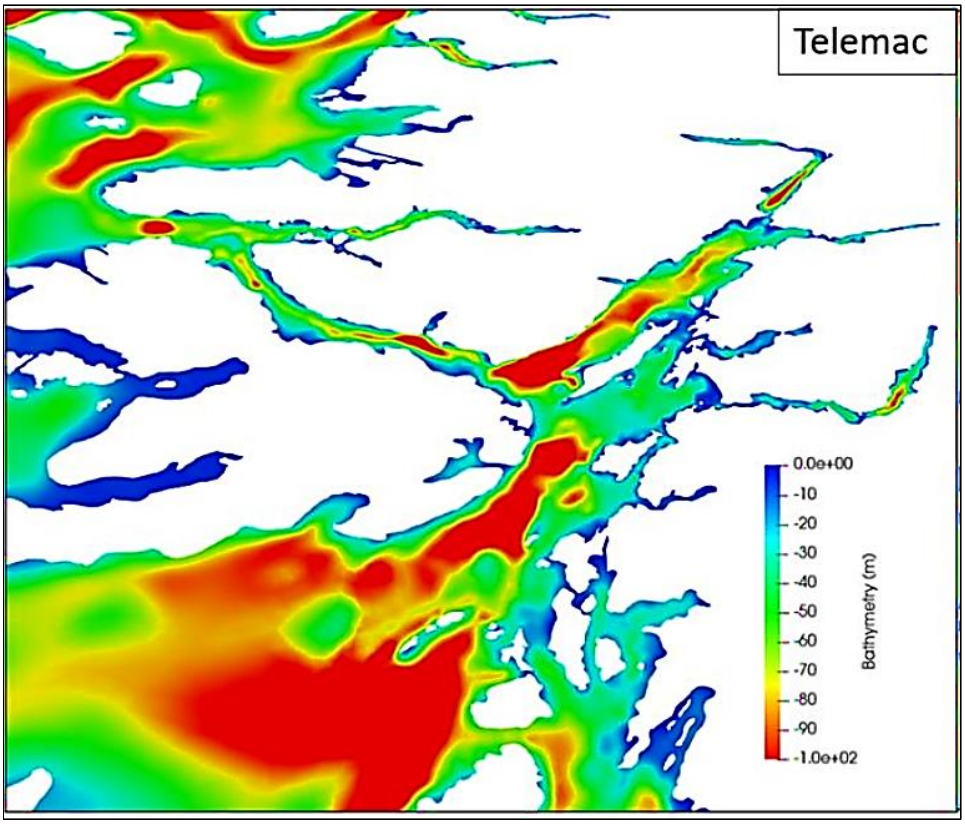

Figure 4 *Sea bed bathymetry in the area around Loch Melfort.*

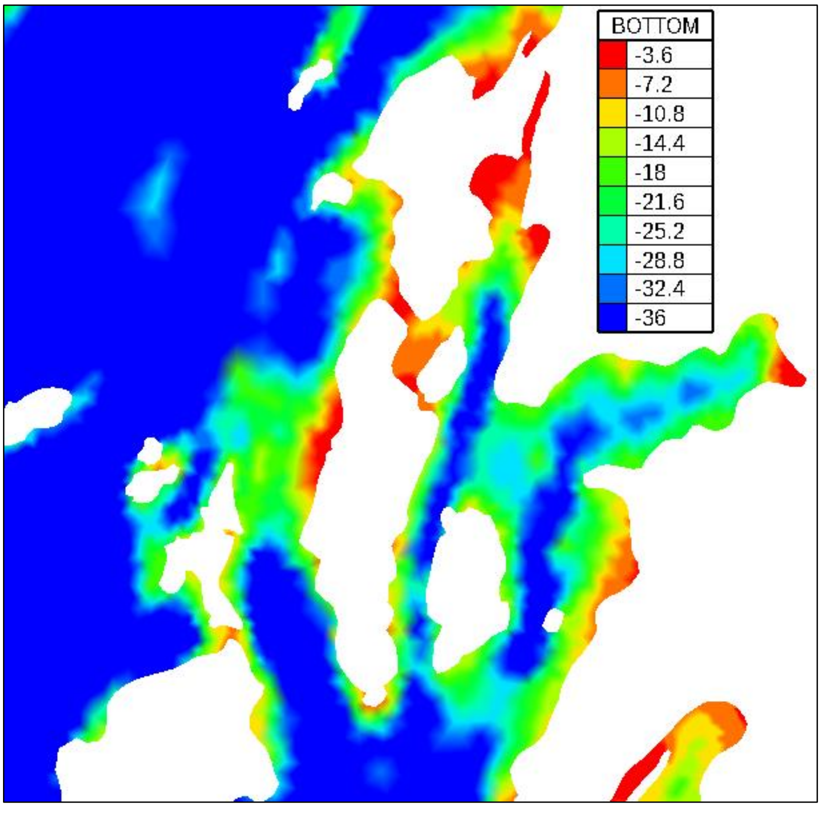

Figure 5 *Zoomed sea bed bathymetry in the area around Loch Melfort.*

2.3 *Meteorology*

Wind forcing on the loch surface is included in the hydrodynamic model based on weather data at 6-hourly intervals covering the period of May 1-15, 2018 [ERA_2024].

2.4 *Freshwater effects in Loch Melfort*

Freshwater inflows at the head of Loch Melfort means that the loch exhibits a degree of stratification. The vertical density gradients produced, combined with air-water heat exchange and tidal forcing, can result in complex flow patterns within the loch which need to be adequately captured in order produce realistic flow fields to transport the larvae particles. The freshwater inflow rates are derived from published data [G2G_2018].

Figures 6-8 show the salinity fields at various heights in Loch Melfort over the run period and demonstrate the degree of stratification in the loch.

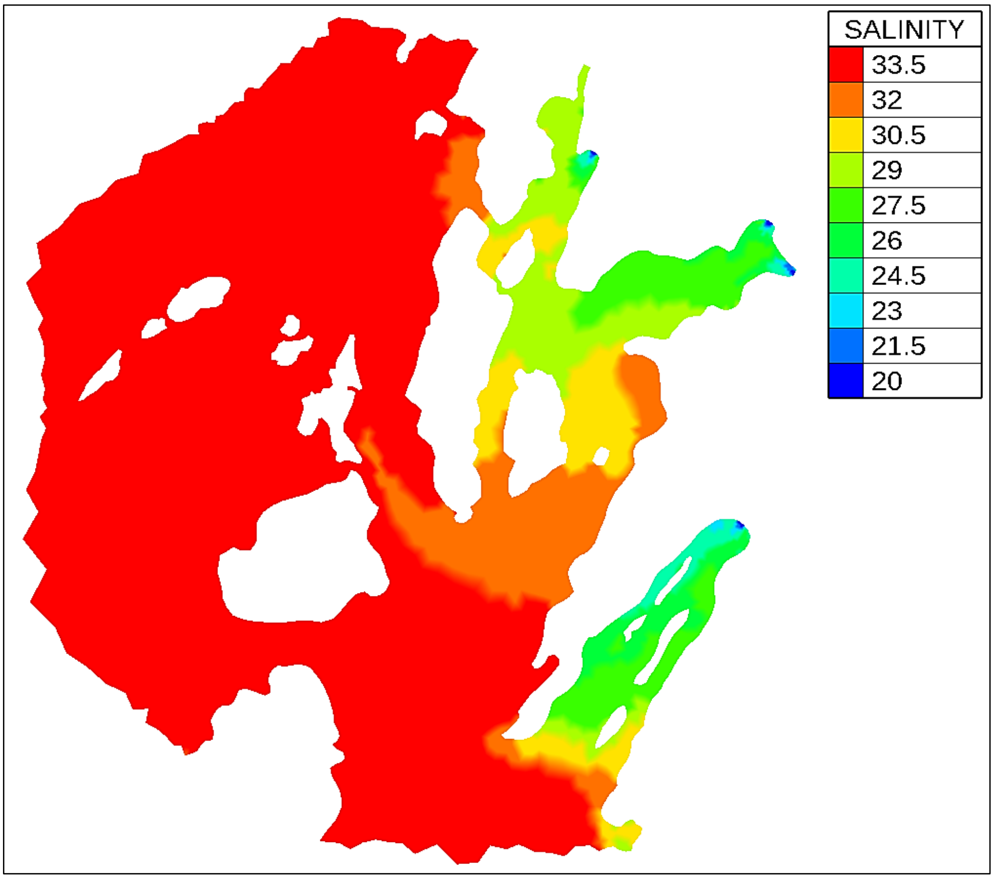

Figure 6 *Snapshot of salinity contours (PSU) in Loch Melfort – near surface.*

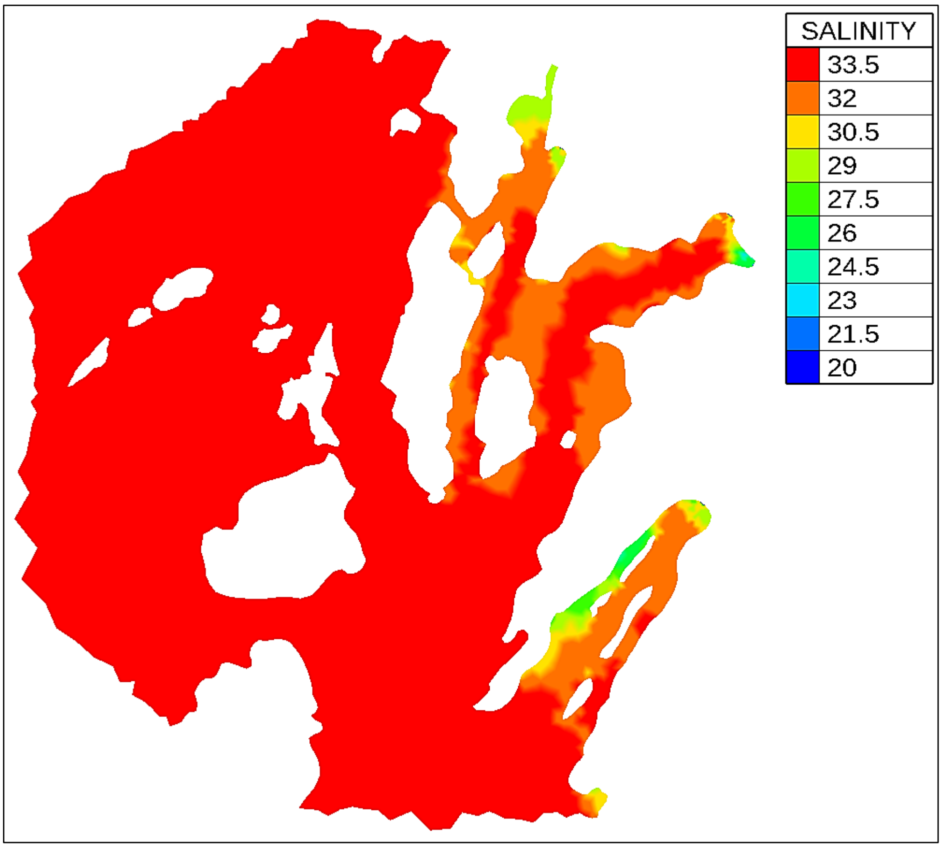

Figure 7 *Snapshot of salinity contours (PSU) in Loch Melfort – 4 m depth.*

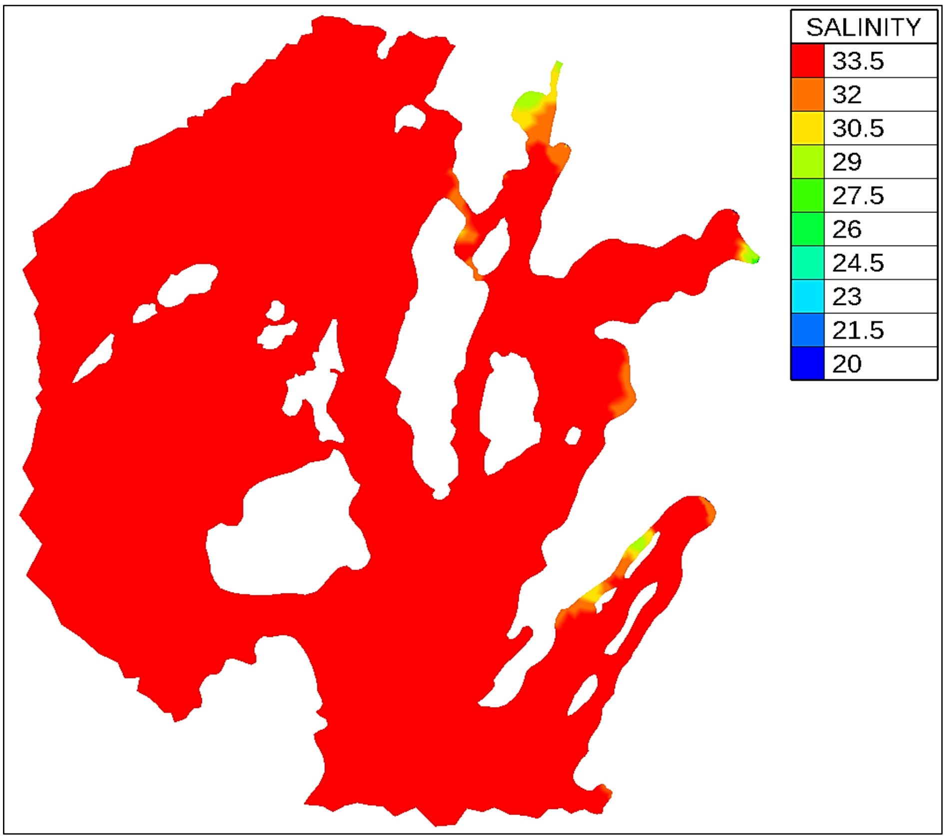

Figure 8 *Snapshot of salinity contours (PSU) in Loch Melfort – near sea bed.*

2.4 *Flow fields*

Figures 9 and 10 show snapshots of the near-surface flow patterns in Loch Melfort on a flood and ebb tide and highlight the complexity of the flows due to the competing effects of tides, wind and stratification.

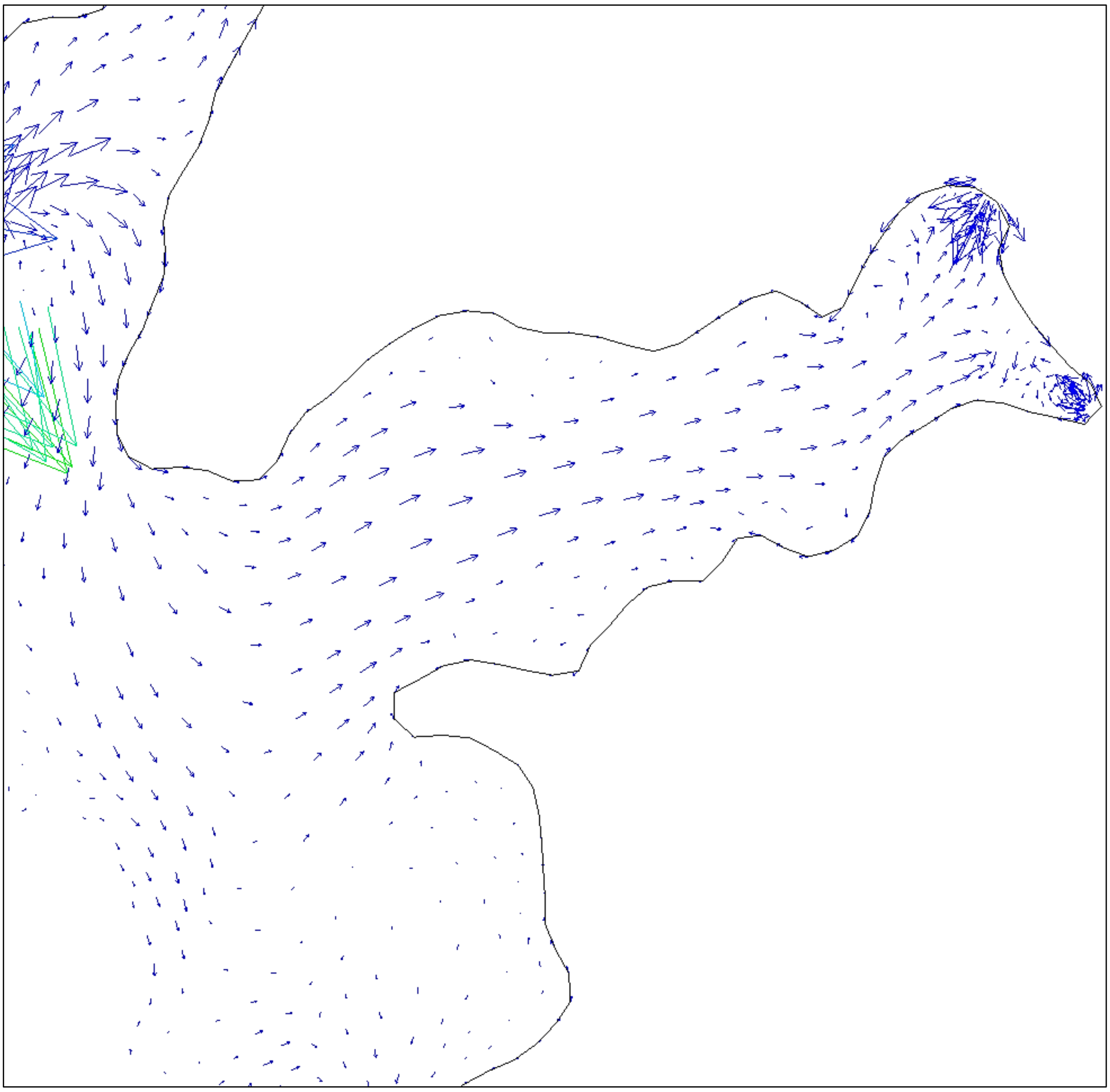

Figure 9 *Snapshot of near-surface flow patterns in Loch Melfort on a flood tide.*

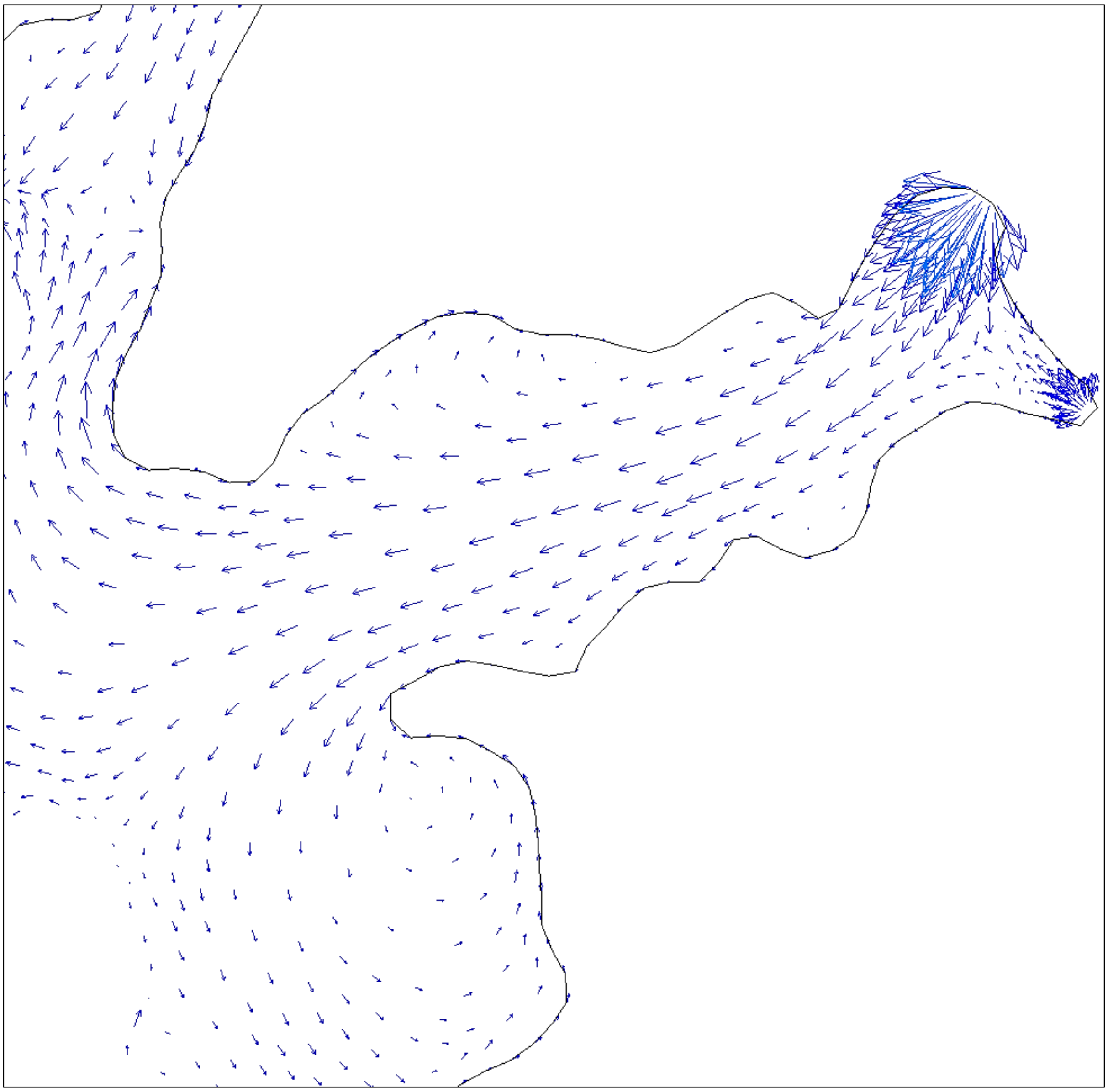

Figure 10 *Snapshot of near-surface flow patterns in Loch Melfort on an ebb tide.*

3 Oyster Larvae Model

3.1 *Model description*

The integrated biological model presented in this report draws on the methods and assumptions used by Scottish and Norwegian modellers working for government agencies, as well as other peer-reviewed research [Johnsen_2020], [Asplin_2020], [Smyth_2016], [North_2008]. A methodology similar to the current SEPA screening model for salmon lice [SEPA_2024] has been employed. In this approach, oyster “larva” particles are released into the marine environment from the 5 release sites in Loch Melfort. Each particle represents a single larva. Details of each release site are shown in Table 1.

Table 1 *Location details of the 5 Oyster Larvae Release Sites*

Name	Longitude (deg)	Latitude (deg)
MEL1	-5.501001	56.265549
MEL2	-5.497089	56.267184
MEL3	-5.487637	56.257051
MEL4	-5.519670	56.247903
MEL5	-5.577937	56.237362

Particles were released continuously at each site at a rate of 20 per hour during the 14-day period from May 1-15, 2018. Initial particle positions were randomly distributed within a volume of radius 10 m and depth 1 m, centred at the lon/lat location of each site. At the end of the 14-day calculation there were approximately 28,000 particles in the system.

In addition to transport by sea currents, particles were given a random movement component, both vertically and horizontally at each time increment to represent turbulence on a subgrid scale. Particles were dispersed in the horizontal using a dispersion coefficient of 0.1 m^2/s and dispersed in the vertical using a dispersion coefficient of 0.001 m^2/s. This is considered a conservative vertical mixing approach [SEPA_2024] for the West Coast of Scotland. The particle integration method used was 4th order Runge-Kutta.

Particles begin their lives as passive trochophores and are transported by sea loch currents during a user-defined maturation time period. When the trochophore maturation time is complete, the particles transform into the veliger biological stage and have the ability to swim upwards during a user-defined number of days. Upwards swimming directs the veligers to the faster-moving water surface layers and affords greater dispersion across the loch. Neither trochophores nor veligers have the ability to deposit on the loch bed.

Finally, particles transform into the pediveliger stage after the maturation period of veligers is reached. Pediveligers have the ability to change swim direction to downwards after a user-set time period and can also sink when a user-defined time period is achieved. Downward swimming/sinking allows the pediveligers to approach the sea bed. When contact is made, the particles will attach at that location, however, they have the ability to be resuspended into the water column if a critical threshold of near-bed shear-stress is reached. For details of the resuspension calculation, see [CLAWS_2024]. Pediveliger particles lose their ability to resuspend after a user-defined time period and are considered to be permanently attached. Pediveligers that fail to attach will expire after a user-defined time period.

3.2 *User-defined settings*

The user-defined settings for each biological stage are shown in Table 2.

Table 2 *User-defined parameters in the oyster larvae model*

Biological stage	Parameter name	Parameter value	Comments
Trochophore	Maturation time to veliger	1 day	Time for passive trochophore stage to mature into upward-swimming veligers
Veliger	Maturation time to pediveliger	3 days	Time for upward-swimming veligers to mature into downward swimming or sinking pediveligers
Veliger	Upward swimming speed	3 mm/s	Based on the paper of [North_2008] but is relevant for oyster species (*Crassostrea virginica*)
Veliger	maximum number of swimming days allowed	3 days	Set to be equivalent to the maturation time to pediveliger
Pediveliger	mortality after day	13 days	Pediveligers expire after 13 days of the 14-day calculation
Pediveliger	Downward swimming or sinking speed	3 mm/s	Based on the paper of [North_2008] but is relevant for oyster species (*Crassostrea virginica*)
Pediveliger	downward swimming after day	6 days	Pediveligers can begin their downward descent to search for a suitable habitat e.g. hard substrata
Pediveliger	sinking after day	7 days	Equivalent to downward swimming but included for completeness
Pediveliger	deposited particles attached permanently after day	10 days	Successfully-deposited particles can no longer resuspend and are permanently attached

Swimming behaviour based on the environmental cue of salinity changes is possible in the oyster larvae model but was not included for the runs presented in this document.

3.3 *Model outputs*

Model outputs are presented in three ways, to categorise how the oyster larvae are likely to be distributed throughout Loch Melfort and beyond:

1. Oyster larvae deposition density (#/m^2) for pediveligers averaged over an 11-day period in May 2018, shown as a heat map.
2. Oyster larvae density (#/m^2) in the water column averaged over an 11-day period in May 2018, shown as a heat map.
3. Graphs of transport success for larvae released from each of the 5 sites. Transport success is defined as the percentage of all particles released from a site that successfully deposit on the sea floor as pediveligers.

4 Results

4.1 *Average deposition and larvae density heat maps*

Figure 11 shows the heat map of the average normalised pediveliger deposited concentration (#/m^2) across Loch Melfort and beyond. The deposition values are normalised with respect to the largest average concentration found in the system.

The results from Fig.11 show that the deposition concentrations are distributed widely across the loch and beyond with significant numbers of larvae observed to exit the loch into the surrounding area.

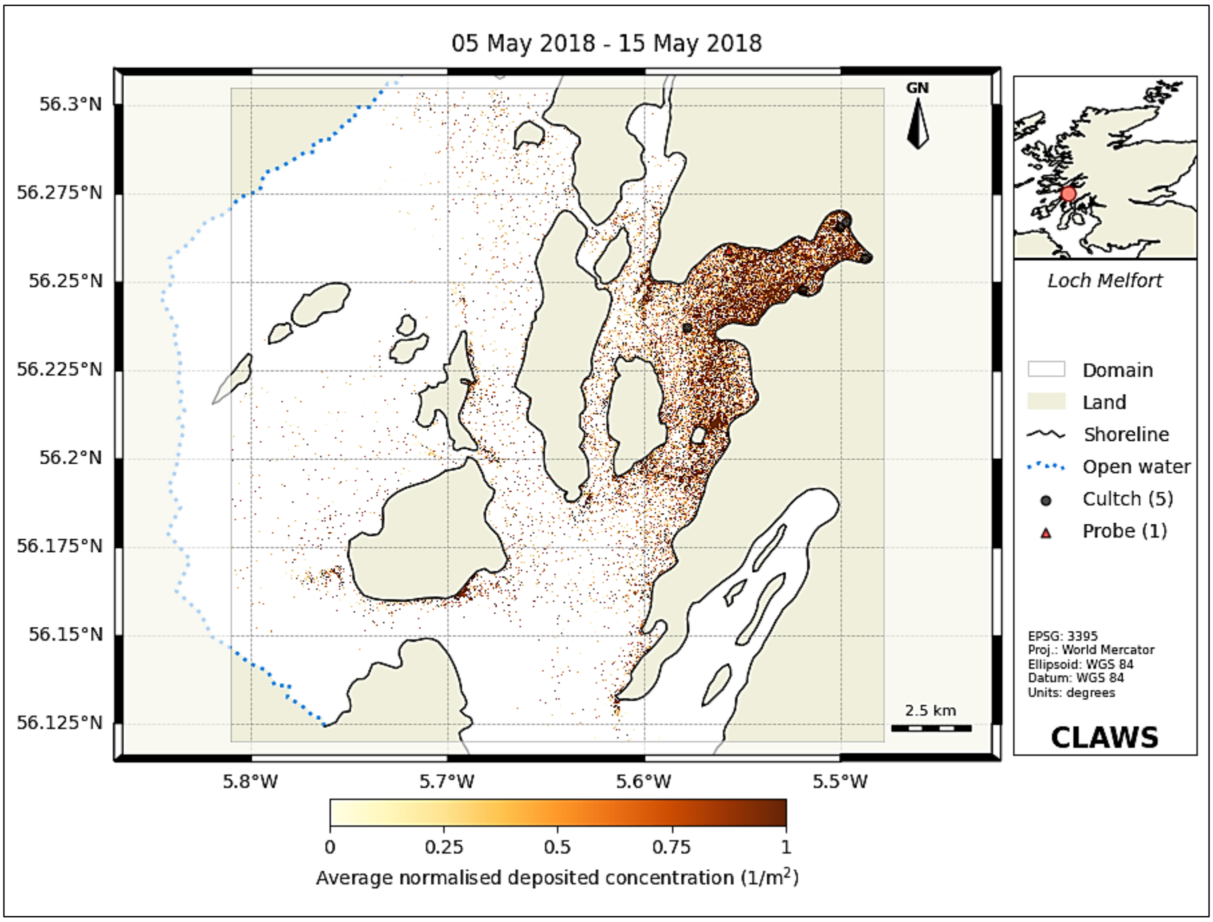

Figure 11 *Average normalised pediveliger deposited concentration (#/m^2) in Loch Melfort over the 11-day period from the 5th-15th May 2018.*

Figures 12-16 show the average oyster trochophore density (#/m^2) in the water column for each release site, averaged over the 11-day period from the 5th-15th May 2018. These images serve to highlight the initial flow paths taken by the nascent larvae from each release location.

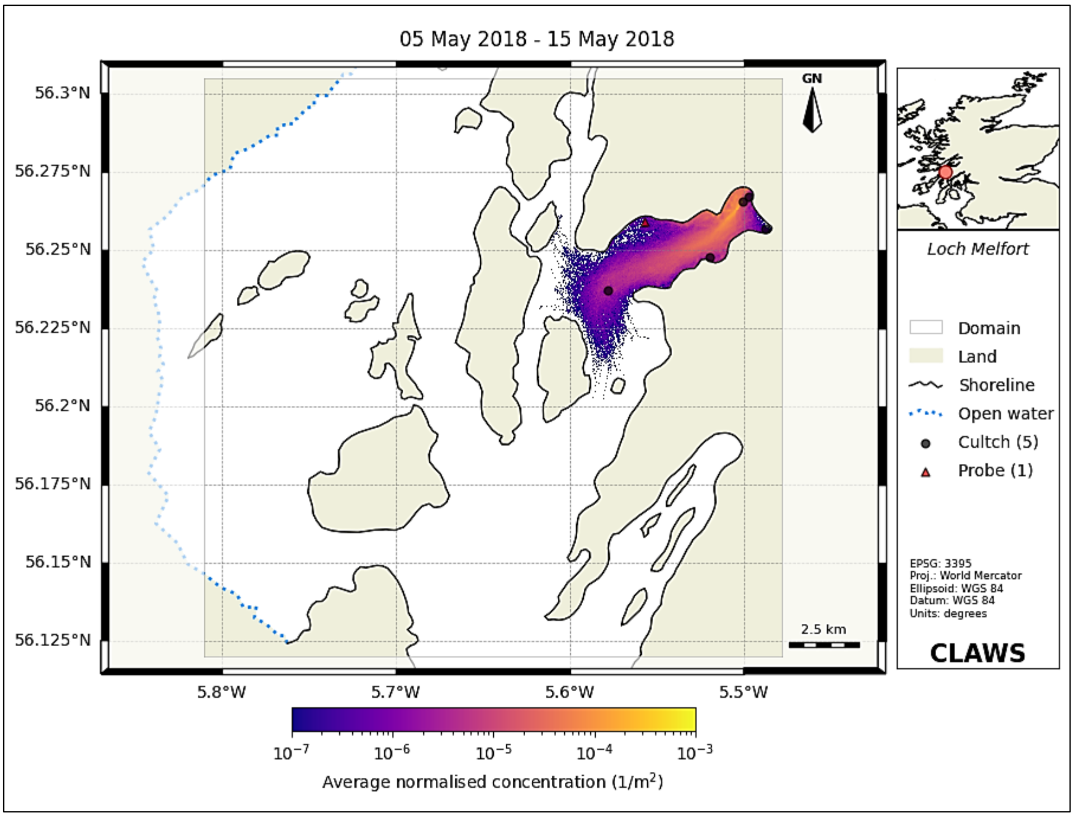

Figure 12 *Average trochophore concentration (#/m^2) in the water column, with release from site MEL1, over the 11-day period from the 5th-15th May 2018.*

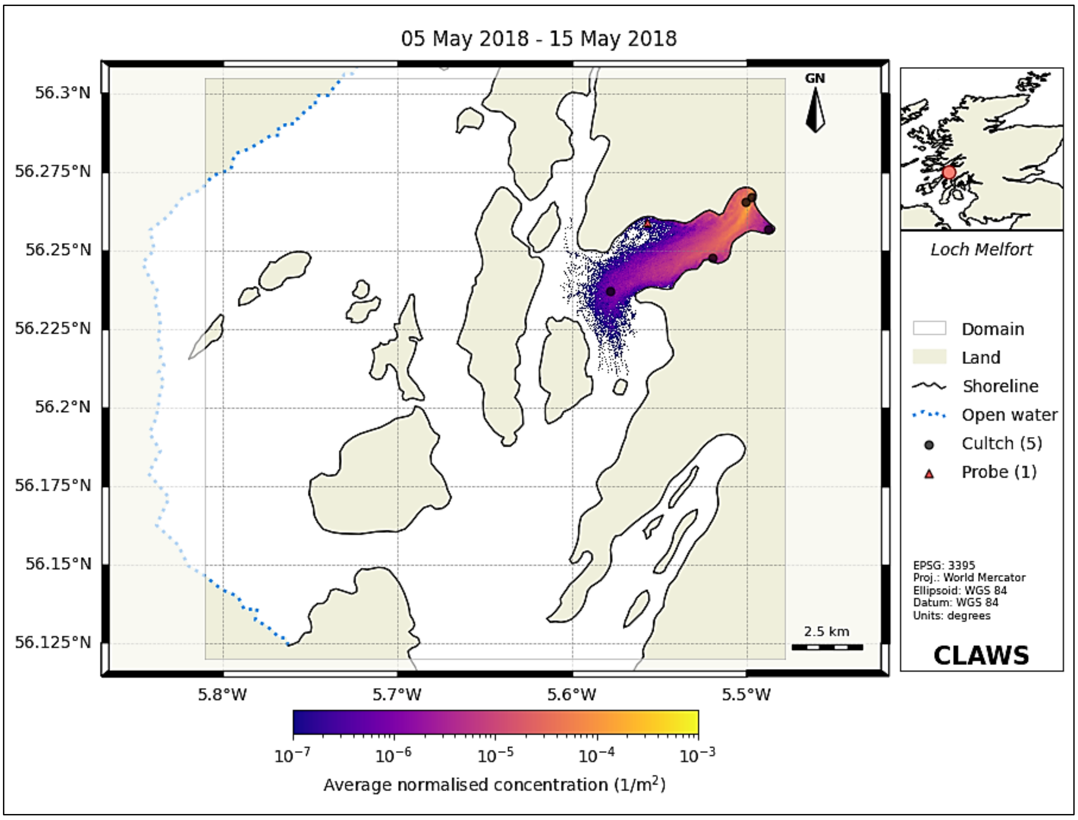

Figure 13 *Average trochophore concentration (#/m^2) in the water column, with release from site MEL2, over the 11-day period from the 5th-15th May 2018.*

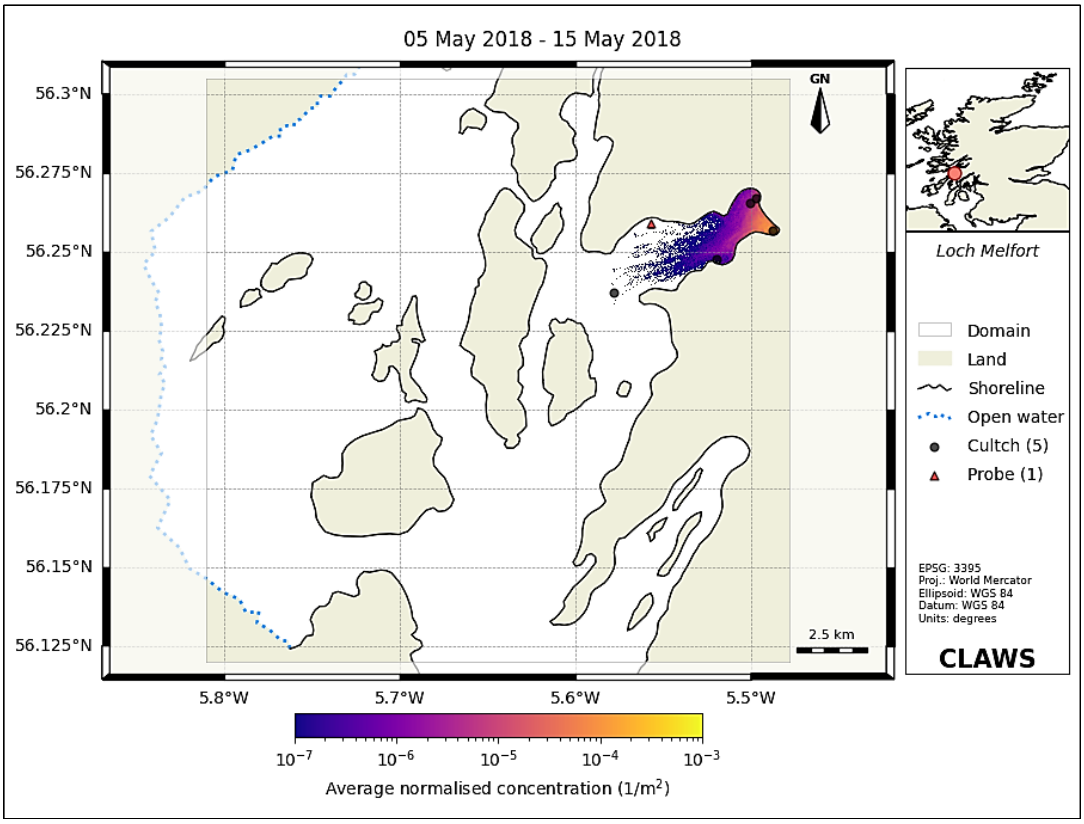

Figure 14 *Average trochophore concentration (#/m^2) in the water column, with release from site MEL3, over the 11-day period from the 5th-15th May 2018.*

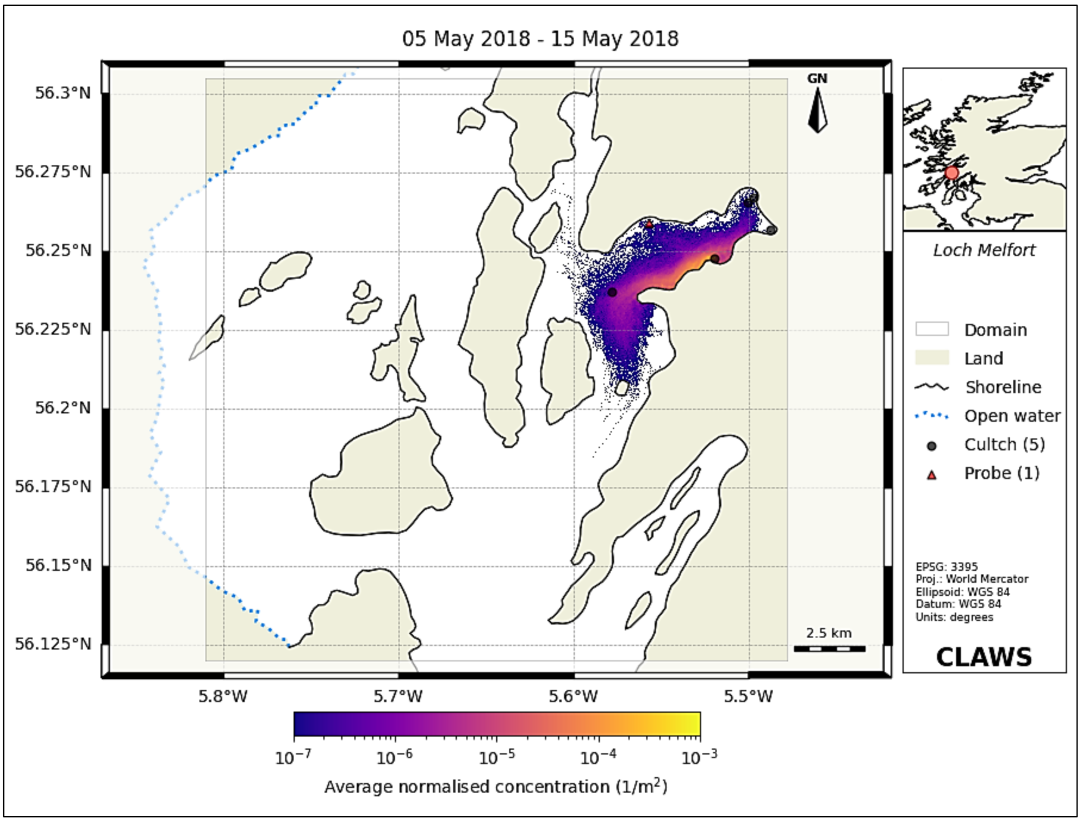

Figure 15 *Average trochophore concentration (#/m^2) in the water column, with release from site MEL4, over the 11-day period from the 5th-15th May 2018.*

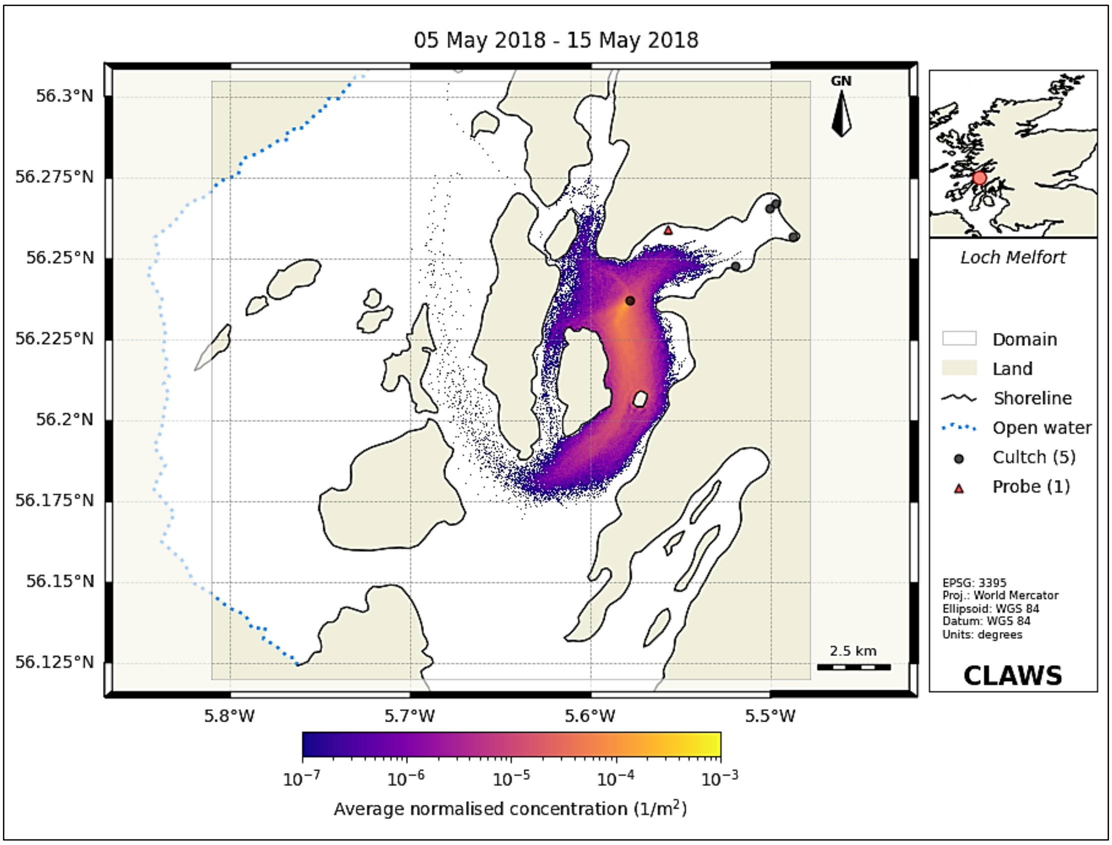

Figure 16 *Average trochophore concentration (#/m^2) in the water column, with release from site MEL5, over the 11-day period from the 5th-15th May 2018.*

In general, the oyster larvae distribution for the trochophore biological stage tends to remain within the confines of Loch Melfort, apart from those released from site MEL5 (Fig. 16). Larvae released from the MEL5 site are likely to be more widely-dispersed into the surrounding marine environment as the loch experiences tidal flushing during the 14-day model run.

Figure 17 shows the average pediveliger concentration (#/m^2) in the water column, with release from all 5 sites, over the 11-day period from the 5th-15th May 2018. It is evident that there is a wider distribution of the pediveliger larvae across the marine setting compared with trochophores. This is likely due to the fact that the trochophore biological stage exists for a much shorter time period compared to the more mature stages. Also, the trochophore stage is passive with regards to swimming. The upward-swimming capability of the veliger and pediveliger stages means that it that they are likely to be transported more widely on the back of the generally faster-moving surface currents in the loch.

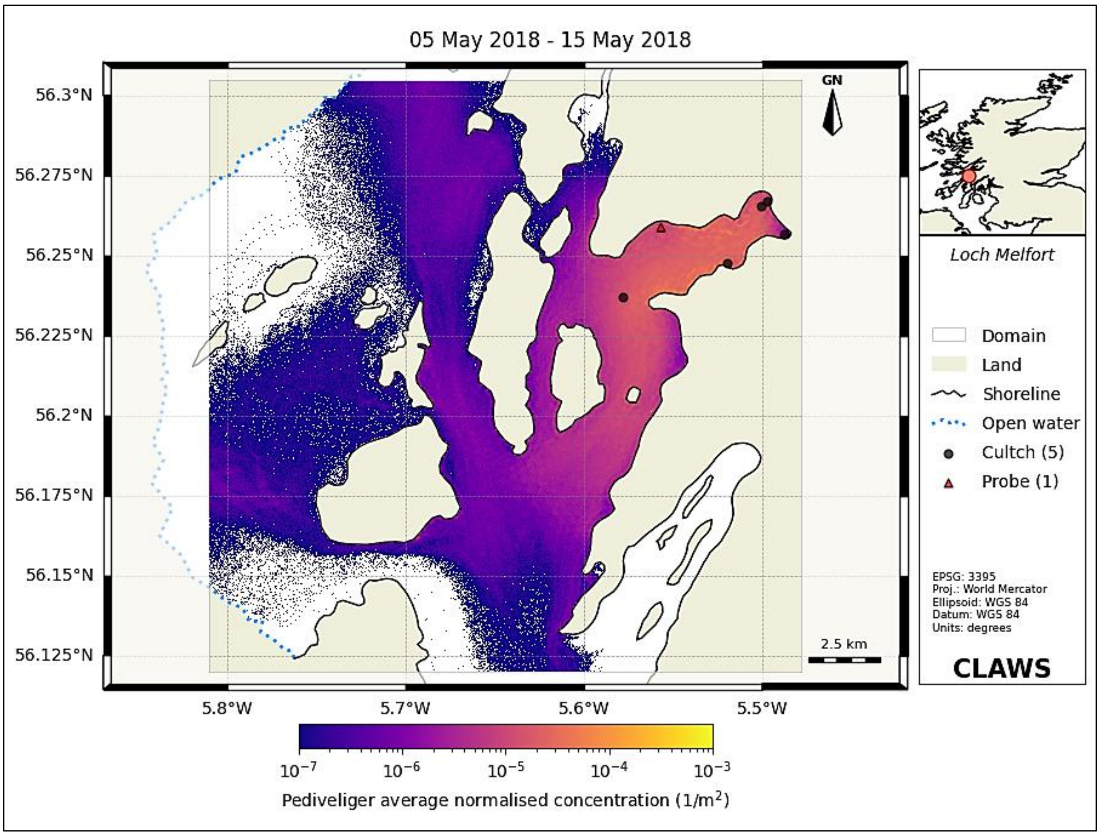

Figure 17 *Average pediveliger concentration (#/m^2) in the water column, with release from all 5 sites, over the 11-day period from the 5th-15th May 2018.*

4.3 *Further data output*

Data from the model runs may be interrogated further to provide additional useful information. Figure 18 shows the plot of transport success for each of the 5 release sites. Transport success is defined as the percentage of all larva particles leaving a site that successfully deposit on the sea floor. The average global transport success across all sites was approximately 50% and this value is comparable with similar levels found in the paper of [North_2008].

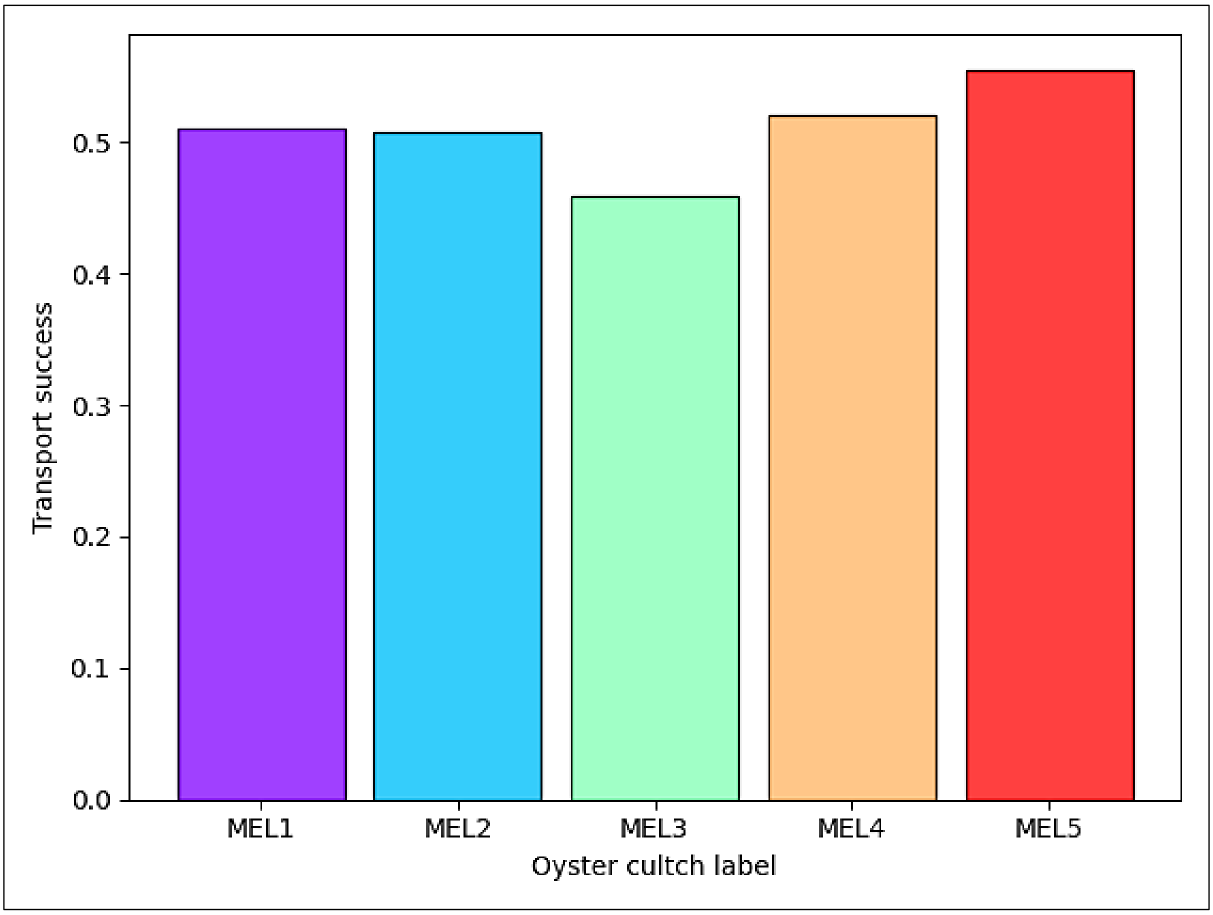

Figure 18 *Bar chart of transport success for the 5 release sites in Loch Melfort.*

4. Conclusions

A multi-stage biological model of oyster larvae (*Ostrea edulis*) has been developed in order to assess their distribution from 5 release sites in Loch Melfort. Tidal, wind and freshwater inflow conditions for May 2018 were considered in a 3D model of the sea loch.

Results for the oyster larvae model show that the average pediveliger deposition concentrations in Loch Melfort are widely distributed within the loch itself, with settling also occurring in the wider marine environment as the loch undergoes tidal flushing during the 14-day model run.

The degree of transport success is predicted to be approximately 50% on average across the 5 release sites.

References

[Asplin_2020], Asplin, L. *et al.*, *The hydrodynamic foundation for salmon lice dispersion modelling along the Norwegian coast*, Ocean Dynamics, 2020 https://doi.org/10.1007/s10236-020-01378-0.

[DOSC_2024], https://digimap.edina.ac.uk/marine - accessed 9th June 2024.

[ERA_2024], https://cds.climate.copernicus.eu/ - accessed 9th June 2024.

[G2G_2018], Bell *et al*., The MaRIUS-G2G datasets: Grid-to-Grid model estimates of flow and soil moisture for Great Britain using observed and climate model driving data. https://rmets.onlinelibrary.wiley.com/doi/abs/10.1002/gdj3.55.

[Johnsen_2020], Johnsen, I. A., Harvey, A., Sævik, P. N., Sandvik, A. D., Ugedal, O.,A˚ dlandsvik, B., Wennevik, V., Glover, K. A., and Karlsen, Ø. *Salmon lice induced mortality of Atlantic salmon during post-smolt migration in Norway.* – ICES Journal of Marine Science, 2020, doi:10.1093/icesjms/fsaa202.

[CLAWS_2024], https://claws-scot.github.io/reports/ - accessed 9th June 2024.

[North_2008], E. W. North, Z. Schlag, R. R. Hood, M. Li, L. Zhong, T. Gross and V. S. Kennedy, *Vertical swimming behavior influences the dispersal of simulated oyster larvae in a coupled particle-tracking and hydrodynamic model of Chesapeake Bay*, Mar Ecol Prog Ser, Vol. 359: 99–115, 2008 doi: 10.3354/meps07317.

[SEPA_2024] https://consultation.sepa.org.uk/regulatory-services/detailed-proposals-for-protecting-wild-salmon/ - accessed 9th June 2024.

[Smyth_2016] David Smyth, Louise Kregting, Björn Elsäßer, Richard Kennedy and Dai Roberts, *Using particle dispersal models to assist in the conservation and recovery of the overexploited native oyster (Ostrea edulis) in an enclosed sea lough*, Journal of Sea Research 108 (2016) 50–59, http://dx.doi.org/10.1016/j.seares.2015.12.009.

[SSM_2024], http://www.marine.gov.scot/themes/scottish-shelf-model - accessed 9th June 2024.